Galaxy Classification

In the past few years, it has become possible to study galaxies at redshifts which are large enough to be cosmologically interesting, *i.e.,* where the lookback time is large enough to allow evolution to be studied. One would expect high-z galaxies to appear somewhat different from galaxies in the local neighborhood. But before we can address this question, we must define what we're looking at. In other words, we need some method of describing the galaxies: a classification scheme.

HUBBLE-SANDAGE CLASSIFICATIONS

[Hubble 1926, *Ap.J.,* **64,** 321]
[Hubble 1936, *Realm of the Nebulae,* Yale University Press]
[Sandage 1961, *The Hubble Atlas of Galaxies,* Carnegie Institution of Washington]
[Sandage 1975, in *Stars and Stellar Systems IX. Galaxies and the Universe,* University of Chicago Press]
[Sandage & Tammann 1981, *A Revised Shapley-Ames Catalog of Bright Galaxies,* Carnegie Institution of Washington]

The most famous classification scheme, of course, is the **Hubble tuning-fork system.** At the bottom of the tuning fork are the ellipticals, which start out with ellipticals, which are typed as En. E0 galaxies are circular on the sky, while E7 galaxies are elongated. Specifically,

$$n = 10(1 - b/a) \tag{4.01}$$

where b/a is the observed axis ratio. At the fork in the diagram are the lenticular galaxies. When Hubble proposed the diagram, these galaxies were only hypothesized. They are now known to occur, and are divided into three types, $S0_1$, $S0_2$, $S0_3$. (The $S0_1$ objects have the smoothest profile with no discernible structure, while the $S0_3$ objects have a structureless envelope, but with narrow dust features within the lens.) After the lenticulars, Hubble divided the diagram into the spirals, Sa, Sb, and Sc, and the barred spirals, SBa, SBb, and SBc. Sandage later sub-divided the Sc galaxies into Sc, Scd, Sd, Sdm, Sm, and Im (with a similar sub-division for the barred galaxies). In addition, he added the additional symbols "(r)," which indicates the presence of an inner ring, "R," which signifies the presence of an outer ring, and "(s)," which says that the spiral arms begin at the end of a bar or are traced to the galaxy's center, rather than the galaxy's inner ring. Needless to say, this scheme isn't very elegant.

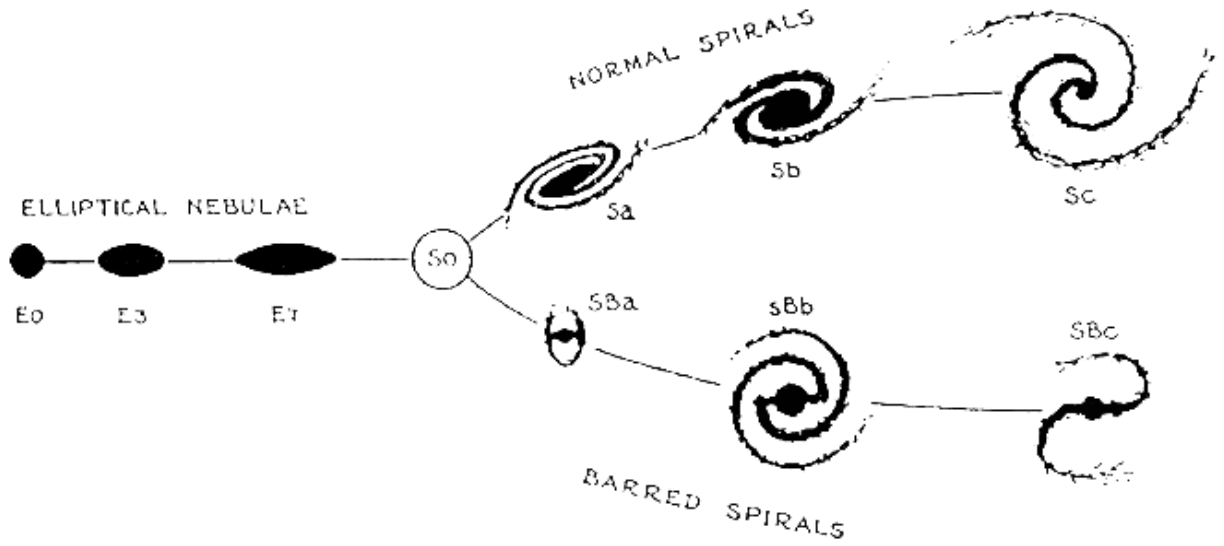

Hubble's original tuning-fork diagram as published in 1936 in his *Realm of the Nebulae.*

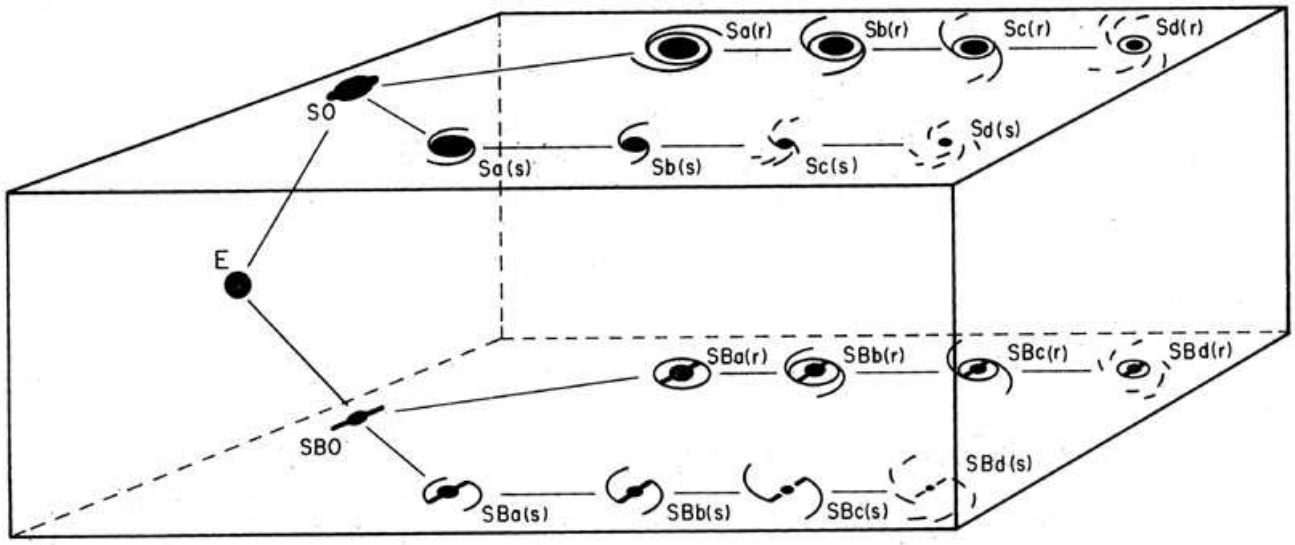

Sandage's extension of the Hubble sequence, as used in the Hubble Atlas and the Revised RSA catalog. This is one of the first attempts at a classification volume.

KORMENDY'S ELLIPTICAL GALAXY MODIFICATION

[Kormendy & Bender 1996, *Ap.J.*, **464,** 119]

Since the ellipticity of an elliptical galaxy is a strong function of its orientation to the line-of-sight, Kormendy & Bender re-ordered the base of the Hubble tuning-fork by isophote shape. Elliptical galaxies whose isophotes are slightly boxy are placed on the far edge of the diagram, while those whose isophotes slightly resemble that of a disk galaxy are placed near the lenticulars. One way that the shape of the elliptical galaxy can be quantified is through

$$r = \left(|x|^{c+2} + \left| \frac{y}{q} \right|^{c+2} \right)^{1/(c+2)} \qquad (4.02)$$

where q is the observed axis ratio. A pure ellipse has $c = 0$; for $c > 0$, the isophotes are slightly boxy (*i.e.*, with a deficit of light along the major and minor axes). For $c < 0$, the isophotes are disky, with an excess of light along these axes.

This ordering is reasonable since the disky ellipticals are also those that have the greatest major axis rotation. However, these isophotal distortions are subtle, and difficult to detect without excellent data.

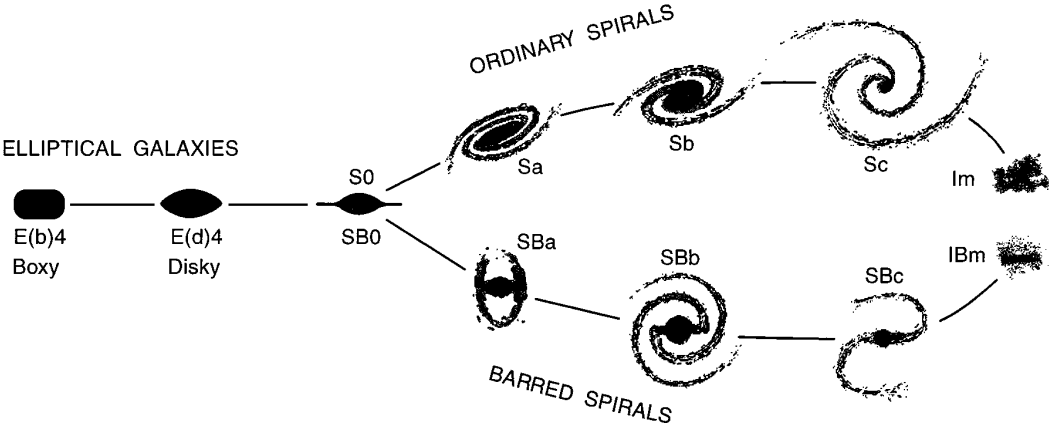

FIG. 1.—Proposed morphological classification scheme for elliptical galaxies. Ellipticals are illustrated edge-on and at ellipticity $\epsilon \simeq 0.4$. The connection between boxy and disky ellipticals may not be continuous (see § 4). This figure is based on the tuning-fork diagram of Hubble (1936). We make three additional modifications: we illustrate the two-component nature of S0 galaxies and label them as barred or unbarred, we call unbarred spirals "ordinary" rather than "normal" (de Vaucouleurs 1959), and we add Magellanic irregulars.

VAN DEN BERGH'S DDO SYSTEM

[van den Bergh 1960, *Ap.J.,* **131,** 215]
[van den Bergh 1960, *Ap.J.,* **131,** 558]

A complementary classification system, which seeks to make a parallel with stellar evolution, is the **DDO** (David-Dunlap Observatory) **Luminosity Classification** for late-type (spiral) galaxies created of van den Bergh. In this scheme, supergiant galaxies with well-developed bright spiral arms and bars have the Roman numeral I (like supergiant stars), and small, low-surface-brightness, irregular galaxies have the Roman numeral V. Of course, since one doesn't usually know a galaxy's distance (except for a rough estimate from its redshift), it is somewhat difficult to estimate the true luminosity. The system therefore assumes that the galaxies with the most well-developed arms are also the most luminous. In the Revised Shapley-Ames Galaxy Catalog, which lists the ~ 1300 brightest galaxies in the sky, Sandage adds the DDO luminosity classification onto his Hubble classification, so, for example, the galaxy NGC 1097 is given the type RSBbc(rs)I-II. (In other words, NGC 1097 is a very large barred Sbc spiral with an outer ring, an inner ring, and arms that begin at the end of the galaxy's bar.)

THE DE VAUCOULEURS SYSTEM

[de Vaucouleurs, de Vaucouleurs, & Corwin 1976, *2nd Reference Catalog of Bright Galaxies,* University of Texas Press]

A more computer-friendly system was devised for the 2nd Reference Catalog of Bright Galaxies by **de Vaucouleurs.** In his system, galaxies are given a numerical **T** designation based on compactness. The most compact elliptical galaxies are assigned $T = -6$; normal ellipticals have $T = -5$, central elliptical (cD) galaxies have $T = -4$, and lenticular galaxies have negative numbers near zero ($-3 < T < -1$). Spiral galaxies start at $T = +1$ for S0/a, and proceed to $T = +10$ for Magellanic Cloud-type irregulars, and $T = +11$ for blue compact irregulars that are sometimes called extragalactic H II regions. In this scheme, there is no difference between a normal spiral and a barred-spiral galaxy.

VAN DEN BERGH'S ANEMIC SPIRALS

[van den Bergh 1976, *Ap.J.*, **206,** 883]

In the 1970's van den Bergh noticed that spiral galaxies in clusters seemed different from those in the field. In particular, many cluster spirals seemed to have less gas and less star-formation than their counterparts in low-density environments. (The S0 galaxies, which are spiral disks without arms or gas, are the extreme example of this phenomenon.) Van den Bergh therefore defined a system where Anemic Spirals occupied the transition between regular spirals and lenticulars. In this system, sequences would be Sa → Aa → S0a, Sb → Ab → S0b, *etc.* For these Anemic galaxies, it is as if something is quenching their active star formation.

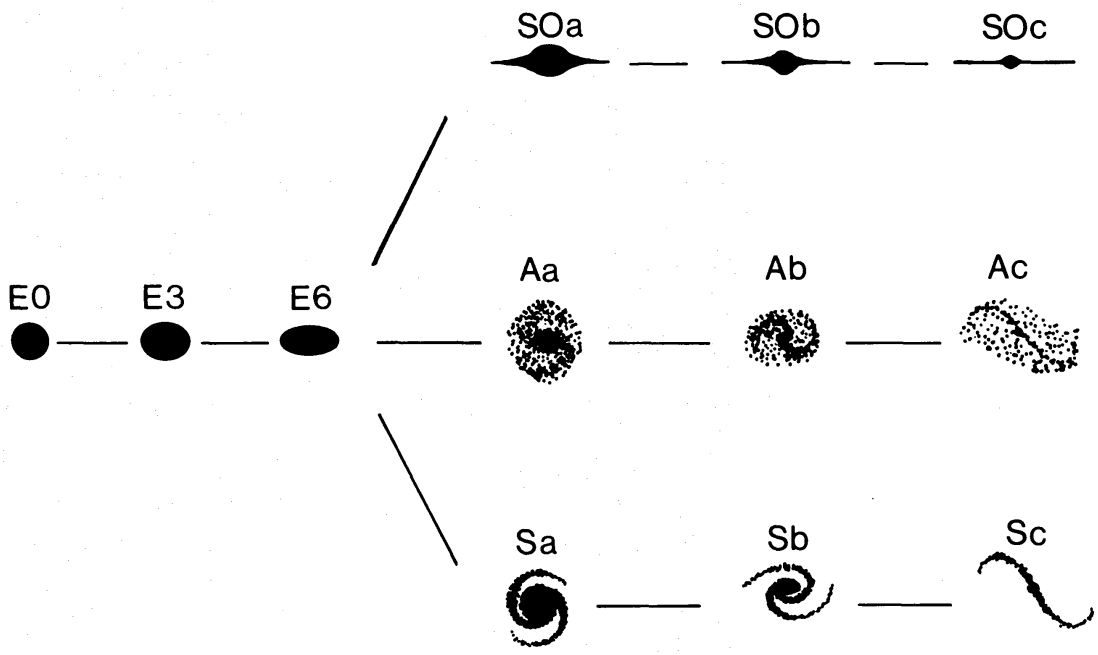

FIG. 2.—Schematic representation of the proposed new galaxy classification system

MORGAN CLASSIFICATIONS

[Morgan 1958, *Pub. A.S.P.,* **70,** 364]
[Morgan 1959, *Pub. A.S.P.,* **71,** 394]
[Morgan, Matthews, & Schmidt 1964, *Ap.J.,* **140,** 35]

An interesting system that is still (partially) with us and has (some) interesting uses is the classification system of **Morgan.** The system has two components, a "concentration" component, and a "form" component. The concentration part of the system reflects the observed correlation between the types of stars present in a galaxy, and how compact the galaxy is. Elliptical galaxies have mostly old stars, and their integrated light is dominated by K supergiants. These objects are also the most condensed systems; *i.e.,* they are highly concentrated. Irregular galaxies with no central mass condensation tend to have younger stars and a corresponding earlier spectral type. Thus, Morgan defined an "a-f-g-k" concentration index based on the spectral classification of stars. For the form index, Morgan chose the (capital) letters "S" for spiral, "B" for barred spiral, "E" for elliptical, "I" for irregular, "E_p" for elliptical peculiar (with dust), "D" for rotationally symmetry without elliptical structure (*i.e.,* a *diffuse* system), "L" for low-surface brightness, and "N" for a compact object with a small, brilliant nucleus (like a Seyfert galaxy). On top of this, Morgan then added a number from 1 to 7 based on apparent inclination: face-on spirals were S1, while highly elongated systems could be S7. Thus, M31 is a kS5 galaxy; M81 is kS4, M33 is fS3, the barred spiral NGC 3351 is fgB1, and the edge-on (Milky Way lookalike) spiral NGC 891 has a Morgan type of gk:S7.

The Morgan system lives on today principally in the designation of "N" galaxies, which are sometimes used to refer to small galaxies with an active galactic nucleus, and through the identification of some galaxies as "cD". The cD designation (which actually came

about 5 years after the original Morgan paper) refers to systems in the centers of clusters which have a elliptical galaxy-like core surrounded by a huge amorphous envelope of stars. These systems are probably the largest collections of stars in the universe; since some cD galaxies have multiple nuclei, they have sometimes been described as "galaxies at lunch."

Quantitative Galaxy Classifications

THE CONCENTRATION INDEX

[de Vaucouleurs 1977, in *Evolution of Galaxies and Stellar Populations,* Yale University Observatory]
[Okamura, Kodaira, & Watanabe 1984, *Ap.J.,* **280,** 7]
[Kent 1985, *Ap.J. Supp.,* **59,** 115]
[Bershady *et al. AJ,* **119,** 2645]

Over the years, various methods have been devised to quantify Morgan's concentration index. In general, these are based on the formula

$$C(r_1, r_2) = \int_0^{r_1} 2\pi r I(r) dr \Bigg/ \int_0^{r_2} 2\pi r I(r) dr \qquad (4.03)$$

For de Vaucouleurs, r_1 and r_2 were radii enclosing 1/4 and 3/4 of the light; for Kent, these fractions were 1/5 and 4/5. For Okamura *et al.*, r_2 represented the radius of the isophote with a V-band surface brightness of 26 mag arcsec^{-2}. All these concentration indices are *highly* correlated; one is just as good as the other, although at present, the Kent radii (20% and 80%) seem to be used most.

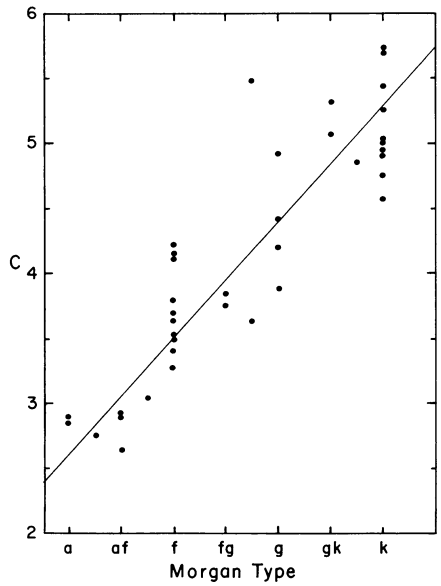

FIG. 9.—Correlation between concentration parameter c and Morgan type. The line drawn is an eyeball fit to the points.

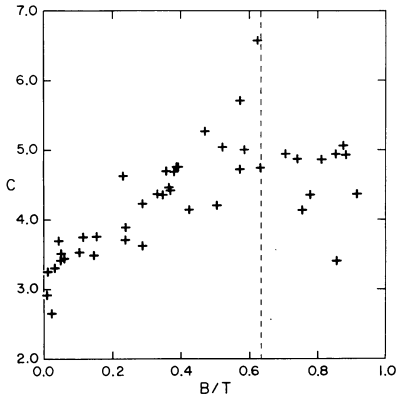

FIG. 10.—Correlation between concentration parameter c and B/T. Dashed line at $B/T = 0.63$ marks the point where bulge/disk decompositions become unreliable.

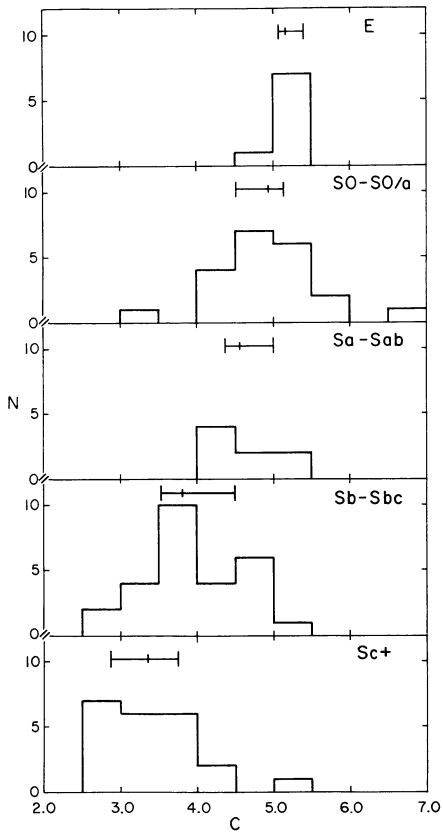

FIG. 11.—Distribution of concentration parameter c as a function of morphological type.

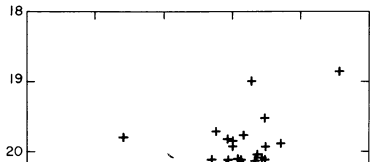

THE SÉRSIC PROFILE

[Sérsic 1968, *Atlas de Galaxias Australes*]

Another often-used parameter of quantitative classification is the Sérsic profile. The surface brightness of a spiral disk typically declines exponentially with $I(r) \propto e^{-r/r_0}$. In contrast, the radial profiles of elliptical galaxies are much more concentrated. Therefore, one can fit the radial profile of a galaxy to

$$I(r) = I(e) \exp\left\{-\kappa\left(\left[\frac{r}{r_e}\right]^{1/n} - 1\right]\right\} \tag{4.04}$$

The variable n is the Sérsic index. If $n = 1$, it is likely that the galaxy has an exponential disk; if $n = 4$, the data are consistent with the profile of an elliptical galaxy.

THE ASYMMETRY INDEX

[Conselice *et al.* 2000, *Ap.J.*, **529,** 886]

A galaxy's asymmetry index is essentially a measure of the difference between it and its mirror image. One takes an image of the galaxy, rotates it by 180 degrees, and then subtracts the rotated image from the original image. After applying a suitable normalization (say, by dividing through by twice the original image), the result is an measure of symmetry: a perfectly symmetric galaxy will have a residual of zero, while a galaxy with perfect antisymmetry will have an asymmetry index of one.

Operationally, the asymmetry index has a number of difficulties. First, one would think that the best way to measure residuals is through the root-mean-square of the difference image (the rms). However, according to Conselice *et al.* (2000), summing the absolute value of all the residuals yields a more robust measurement. Second, the asymmetry index requires knowing the exact position of the center of the galaxy ahead of time. Since this is difficult to know for faint objects, one usually computes asymmetry indexes for many, many possible centers, and sees which center produces the best (least asymmetric) result. Finally, even a perfectly symmetric galaxy will have *some* residual, due simply to photon noise. To estimate the importance noise in the measurement, one performs the identical measurement on a nearby region of blank sky and measures its asymmetry. Hence the final equation for asymmetry is

$$A = \min\left(\frac{\sum |I_0 - I_\phi|}{\sum |I_0|}\right) - \min\left(\frac{\sum |B_0 - B_\phi|}{\sum |I_0|}\right) \qquad (4.05)$$

where I_0 and I_ϕ represent the counts of the original and the rotated image, B_0 and B_ϕ, the counts in a nearby region of sky, the summation is taken over all the pixels in the galaxy, and the minimization instruction reflects the fact that many trials have been

run with different values for the galaxy (and blank sky) centroid. Note that in this formulation, asymmetry can theoretically range from zero to two.

In practice, the asymmetry index can change dramatically as one obtains better of data. On short exposures, faint, asymmetric features may be invisible; on a long exposure, they may dominate. Also, a galaxy may be symmetric overall, but have a moderately large asymmetry value due to the contribution of individual H II regions. So in some cases, it is better to run a smoothing algorithm on the image before calculating asymmetry.

THE CLUMPINESS (OR SMOOTHNESS) INDEX

[Conselice *et al.* 2000, *Ap.J.*, **529,** 886]

One measure of the importance of small-scale features (such as H II regions) is to take an image of a galaxy, smooth it with a Gaussian kernel with width σ, and then subtract this smoothed image from the original. In other words,

$$S = 10 \times \sum \frac{(I_0 - I_\sigma) - B}{I_0} \tag{4.06}$$

where I_0 and I_σ are the pixel values in the original and smoothed galaxy image, B represents the pixel values in a blank region of sky (equal in size to the galaxy image), and the summation is taken over all the pixels of the galaxy. In practice, this procedure will produce odd artifacts near the bright centers of galaxies (due to finite sampling and the interaction between a symmetric kernel and an asymmetric galaxy), so regions near a galactic nucleus are usually excluded. Also, a hard floor is used, so that at no place does the subtraction produce a negative value. Finally, one should note that this type of formulation is sensitive to kernel size – wider Gaussians will produce more clumpiness than narrow Gaussians – so you need to define what type of structure you want to investigate ahead of time.

THE GINI COEFFICIENT

[Lorentz 1905, *J. Am. Stat. Assoc.*, **9,** 209]
[Abraham *et al.* 2003, *Ap.J.*, **588,** 218]

Imagine a perfectly uniform galaxy. In an image of this galaxy, every pixel would have the same value, and a plot showing the cumulative amount of light (normalized to one) versus the fraction of pixels in the galaxy would be a straight line with slope 1. Alternatively, consider a galaxy with a very faint body but an extremely bright central nucleus. In this case, if you rank the pixels in order of brightness and perform the same plot, the line would be close to zero, and then shoot up to one right near the end. The Gini coefficient measures the difference in the area under the curve between these two cases. Mathematically, if I_i is the value of the i-th pixel of an image that contains n pixels, then

$$G = \frac{1}{2\bar{I}n(n-1)} \sum_{i=1}^{n} \sum_{j=1}^{n} |I_i - I_j| \tag{4.07}$$

or, if one first sorts the pixels in increasing order,

$$G = \frac{1}{\bar{I}n(n-1)} \sum_{i=1}^{n} (2i - n - 1)\, I_i \quad (n > 2) \tag{4.08}$$

(The proof of this last equation is left to the student who likes to do lots and lots of math.)

The Gini coefficient is similar to the concentration index, C, as it measures how different the galaxy is from a uniform collection of stars. As such, C and G are well-correlated.

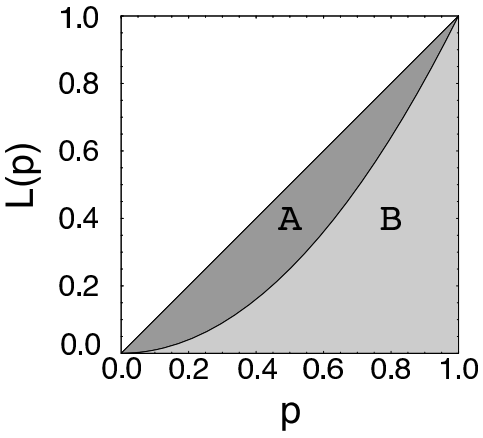

FIG. 1.—Geometric interpretation of the Gini coefficient based on the Lorenz curve. The x-axis corresponds to the quantile of the distribution, and the y-axis corresponds to the cumulative proportion. The Lorenz curve for a perfectly equal distribution corresponds to the diagonal line of equality. In the figure, a schematic Lorenz curve divides the area beneath the line of equality into two areas, A and B. The greater the deviation of a measured Lorenz curve from the line of equality, the greater the inequality. The Gini coefficient corresponds to the ratio of area A to the total area under the diagonal A + B.

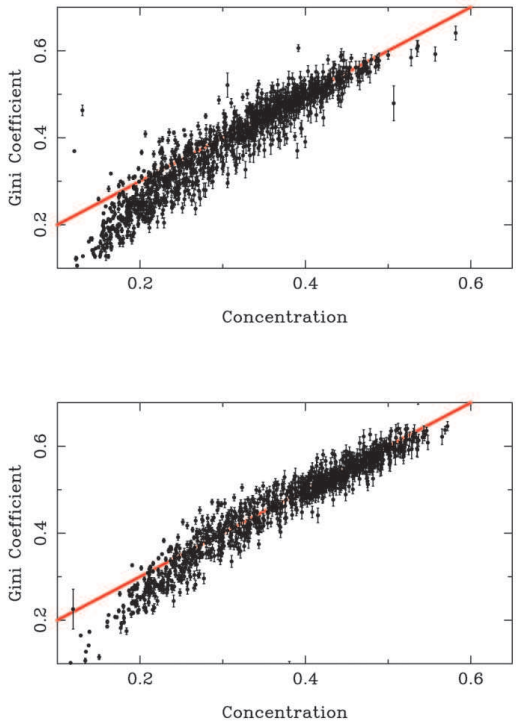

FIG. 3.—Gini coefficient vs. central concentration for the g-band sample (*top*) and i-band sample (*bottom*). The solid line corresponds to unity slope. While the overall slope of the distributions remains similar in both bands, the g^*-band sample exhibits slightly greater scatter, and more high-G, high-C systems are seen in the i^* band. Note that the galaxies span a broad range of morphologies, from pure disk systems at low C to highly centrally concentrated pure $R^{1/4}$-law elliptical galaxies at high C.

MOMENTS

[Lotz *et al.* 2004, *A.J.*, **128,** 163]

A traditional way of classifying objects is through the use a moments. An objects' first-order moment is just its weighted center, *i.e.,* its center of gravity.

$$x_c = \frac{\sum f_i x_i}{\sum f_i} \qquad y_c = \frac{\sum f_i y_i}{\sum f_i} \tag{4.09}$$

The second order moment measures the dispersion about these means

$$m_2 = \sum \frac{f_i \left[(x_i - x_c)^2 + (y_i - y_c)^2\right]}{f_i} \tag{4.10}$$

The third order moment (the skewness) is a measure of asymmetry, and the fourth order moment (the kurtosis) reflects the relative peakedness/flatness of a distribution. In other words, the nth moment of a distribution is defined as

$$m_n = \sum \frac{f_i \left[(x_i - x_c)^n + (y_i - y_c)^n\right]}{f_i} \tag{4.11}$$

The more concentrated a galaxy is, the larger its even-numbered moments; the more asymmetric a galaxy is, the larger (in absolute value) is its odd-numbered moments. Skewness (3rd order) or kurtosis (4th order) are often used to discriminate real objects from cosmic rays on CCD frames; the second order moment is sometimes used in galaxy classification. Also, to improve the robustness of the measurement, one usually restricts the calculation to certain regions of the galaxy; for instance, Lotz *et al.* suggest sorting the pixels and only using the brightest pixels that contain 20% of the galaxy's flux.

Nearby Galaxy Catalogs

The Shapley-Ames Catalog (RSA). A 1932 catalog containing 1246 galaxies with photographic magnitudes $m_{pg} \lesssim 13.2$. The Revised Shapley-Ames Catalog was compiled by Sandage & Tammann in 1981 and is an all-sky catalog containing 1249 galaxies with $m_B \leq 13$. The catalog contains positions, B-magnitudes, Hubble types, and redshifts.

The Reference Catalog of Galaxies (RC3). This catalog was compiled by de Vaucouleurs, and contains positions, estimated magnitudes, sizes, and redshifts (if available).

RC1 (1964): 2599 galaxies
RC2 (1976): 4364 galaxies
RC3 (1991): 23,024 galaxies

RC3 is complete to $m_{pg} \lesssim 15.5$ and $z < 15,000$ km s^{-1} (11,897 galaxies).

The Uppsala General Catalog (UGC). This catalog, compiled by Nilson (1973) from digital copies of the original Palomar Sky Survey, contains 12,921 galaxies with $m \lesssim 14.5$ or diameters $D > 1'$. The catalog contains positions, types, magnitudes, sizes, and redshifts (if available).

The Zwicky Catalog. These are 6 volumes of listings of galaxies with $m \lesssim 15.5$. Galaxies are named by volume number and field.

The Morphological Catalog of Galaxies (MCG). Voronstov-Vel'yaminov compiled the positions of magnitudes of $\sim 29,000$ galaxies with $m \lesssim 15.1$. It also gives the galaxies' MCG morphological types. The MCG classification scheme is far too complex to be understood by mere mortals.

The Galaxy Luminosity Function

[Schechter 1976, *Ap.J.*, **203,** 297]

One of the key pieces in the study of galaxies and galaxy evolution is the galaxy luminosity function. Traditionally, the number of galaxies versus absolute luminosity (or absolute magnitude), ϕ, has been parameterized by the Schechter luminosity function

$$\phi(L)dL = \phi^* \, (L/L^*)^\alpha \, e^{-L/L^*} d(L/L^*) \tag{5.01}$$

Note the form of the equation. For faint galaxies with $L \ll L^*$, the exponential term goes to 1, and the luminosity function asymptotes to a power law with slope α. At the bright end, where $L > L^*$, the exponential term dominates, and the number of galaxies rapidly goes to zero. L^* is therefore sometimes called the "knee" of the function, and represents the luminosity of a typical "bright" galaxy. (It is often quoted in terms of magnitudes, *i.e.*, M^*.) The variable ϕ^* normalizes the function and defines the overall density of galaxies in the universe. Note that this function (without ϕ^*) does *not* normalize to one. So if L^* or α changes, so does ϕ^*.

If one writes the Schechter function in terms of magnitude, instead of luminosity, the equation is

$$\phi(M)dM = 0.921\phi^* X^{\alpha+1} e^{-X} dM \tag{5.02}$$

where

$$X = 10^{0.4(M^*-M)} \tag{5.03}$$

(The proof is left to the student who likes to doodle while taking notes.)

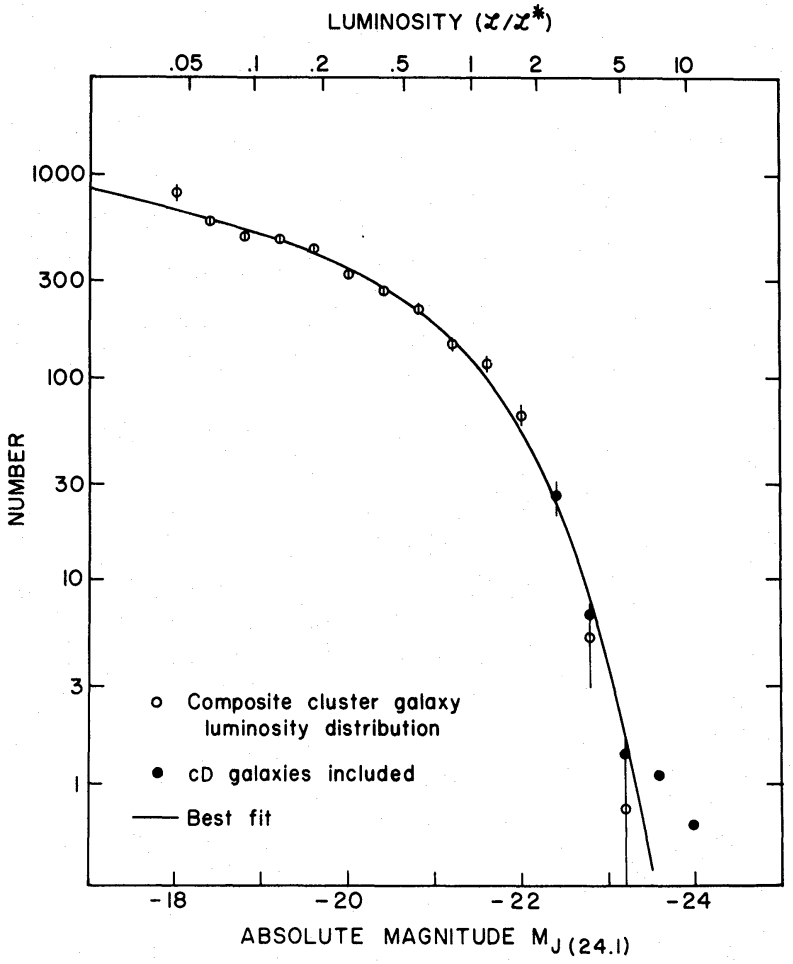

FIG. 2.—Best fit of analytic expression to observed composite cluster galaxy luminosity distribution. Filled circles show the effect of including cD galaxies in composite.

Note the excess of extremely bright galaxies. These are the cD galaxies; this departure from the Schechter function suggests that the formation of these objects is somewhat different from the rest of the galaxy population.

Properties of the Schechter Function

Typical numbers for the key parameters of the Schechter function are $\alpha \sim -1$, $M^* \sim -21$, and $\phi^* \sim 0.002$ galaxies per cubic Megaparsec. To calculate the total number of galaxies implied by the function, one can simply integrate the function. If we let $t = L/L^*$, then $dL = L^* dt$ and

$$N = \int_0^\infty \phi(L) dL = \int_0^\infty \phi^* L^* t^\alpha e^{-t} dt \tag{5.04}$$

This is called an Euler integral, which for the case of $\alpha \geq -1$ has the solution

$$N = \phi^* L^* \int_0^\infty t^\alpha e^{-t} dt = \phi^* L^* \Gamma(\alpha + 1) \tag{5.05}$$

where Γ is the gamma function. However, if $\alpha < -1$ (which is usually the case), the gamma function is undefined, and the implied number of galaxies is infinite. Although this may seem uncomfortable (since there may be many small galaxies under your desk), it is not a terrible problem, since the total luminosity implied by the function will still be finite, *i.e.*,

$$\int_0^\infty \phi(L) L dL = \int_0^\infty \phi^* L (L/L^*)^\alpha e^{-L/L^*} d(L/L^*) = \phi^* L^* \Gamma(\alpha + 2) \tag{5.06}$$

Obviously, to count the number of galaxies down to some limiting magnitude, one can simply change the lower limit on equation (5.04). The integral then becomes the complement of an incomplete gamma function (which is a subset of something called a confluent hypergeometric function). There are tables, expansions, and approximations for such function (see the *Handbook of Mathematical Functions* by Abramowitz & Stegun), but it's usually just easier to integrate the curve numerically.

Schechter Functions for Galaxy Types

[Efstathiou, Ellis, & Peterson, 1988, *MNRAS*, **232,** 431]
[Postman & Geller 1984, *Ap.J.*, **281,** 95]
[Marzke *et al.* 1994, *A.J.*, **108,** 437]
[Croton *et al.* 2005, *MNRAS*, **356,** 1155]

The luminosity function of galaxies changes with galaxy type: elliptical galaxies have a brighter value of M^* than irregulars. The early-type galaxies also have a flatter faint-end slope than the irregulars.

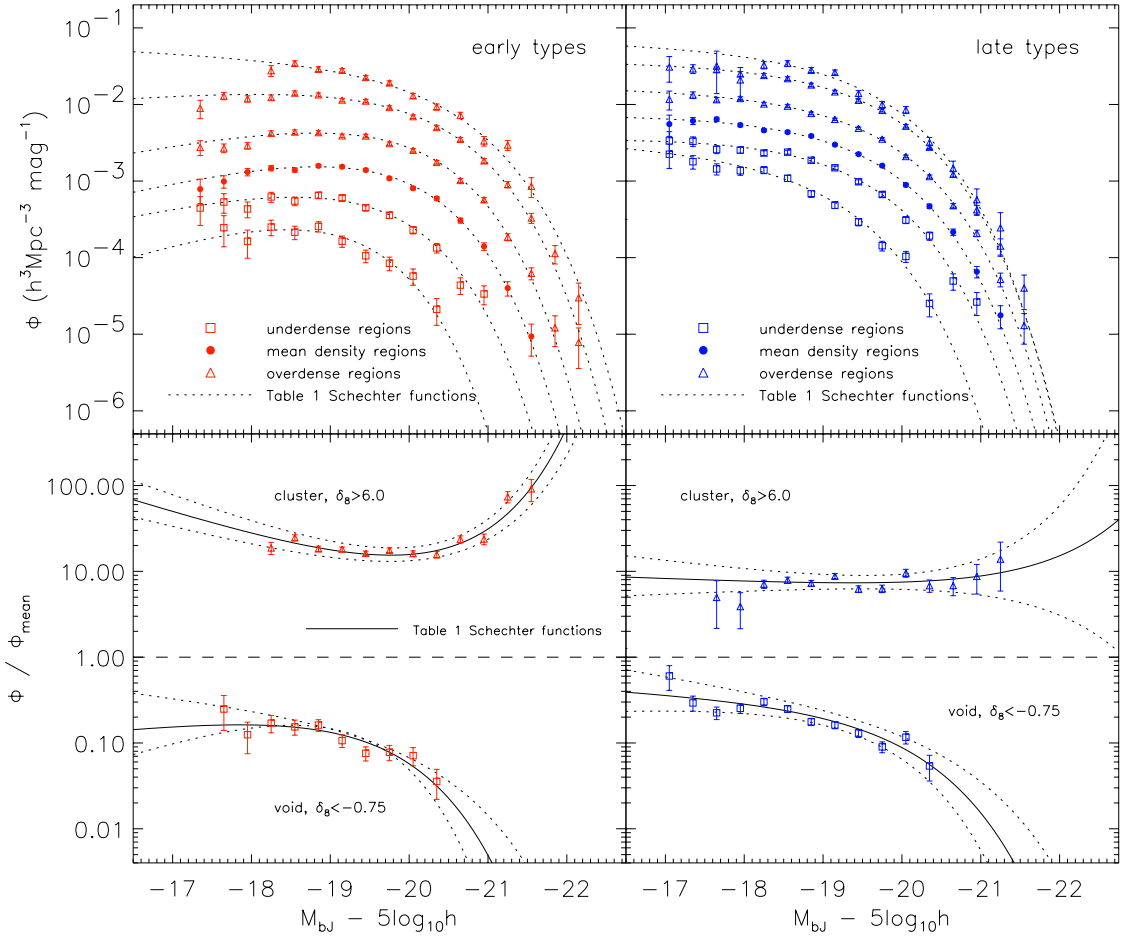

Figure 4. Comparing both the (top) absolute and (bottom) relative distributions of (left) early-type galaxies in various density environments, and (right) late-type galaxies in various density environments. In the bottom panels the luminosity functions have again been normalized to the mean (each to their respective type) as in Fig. 3 (note that the shape of the mean for each type is very similar to that shown in Fig. 1). Here the solid lines and bounding dotted lines show the appropriate Table 1 Schechter functions normalized to the mean Schechter function and 1σ uncertainty.

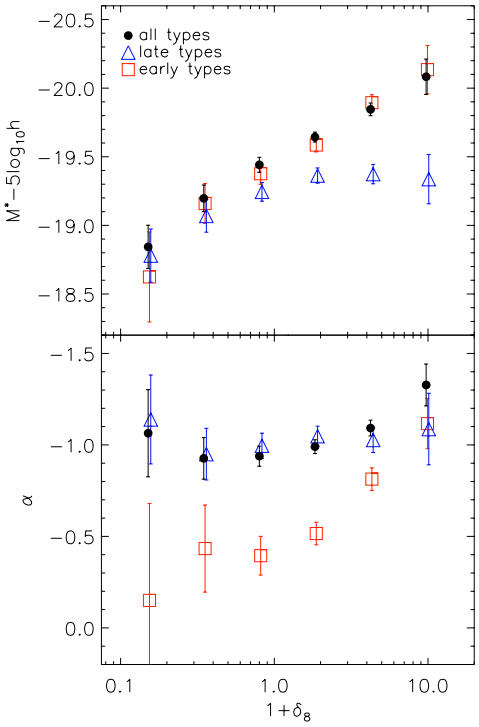

Figure 7. The maximum likelihood Schechter function M^* and α parameters for each of the six density contrast regions in Table 1 (Figs 3 and 4). Each panel shows the results for individual samples split by spectral type (early/late) and for both types combined.

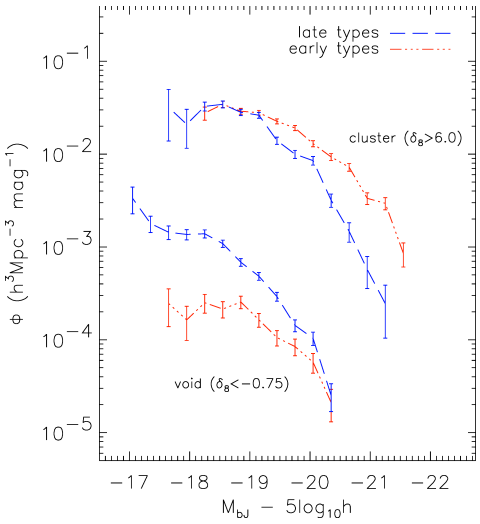

Figure 5. A direct comparison of the early- and late-type galaxy populations in the cluster environment (top two luminosity functions) and void regions of the survey (bottom two luminosity functions). The void population is composed almost exclusively of faint late-type galaxies, while in the cluster regions the galaxy population brighter than $M_{bJ} - 5\log_{10} h = -19$ consists predominantly of early types.

As the figures show, the normalization of the Schechter function for the different types of galaxies is a strong function of environment. In other words, the ratios of ellipticals to spirals is a strong function of the galactic space density. Ellipticals (and lenticulars) generally live in clusters; in the field, spirals dominate.

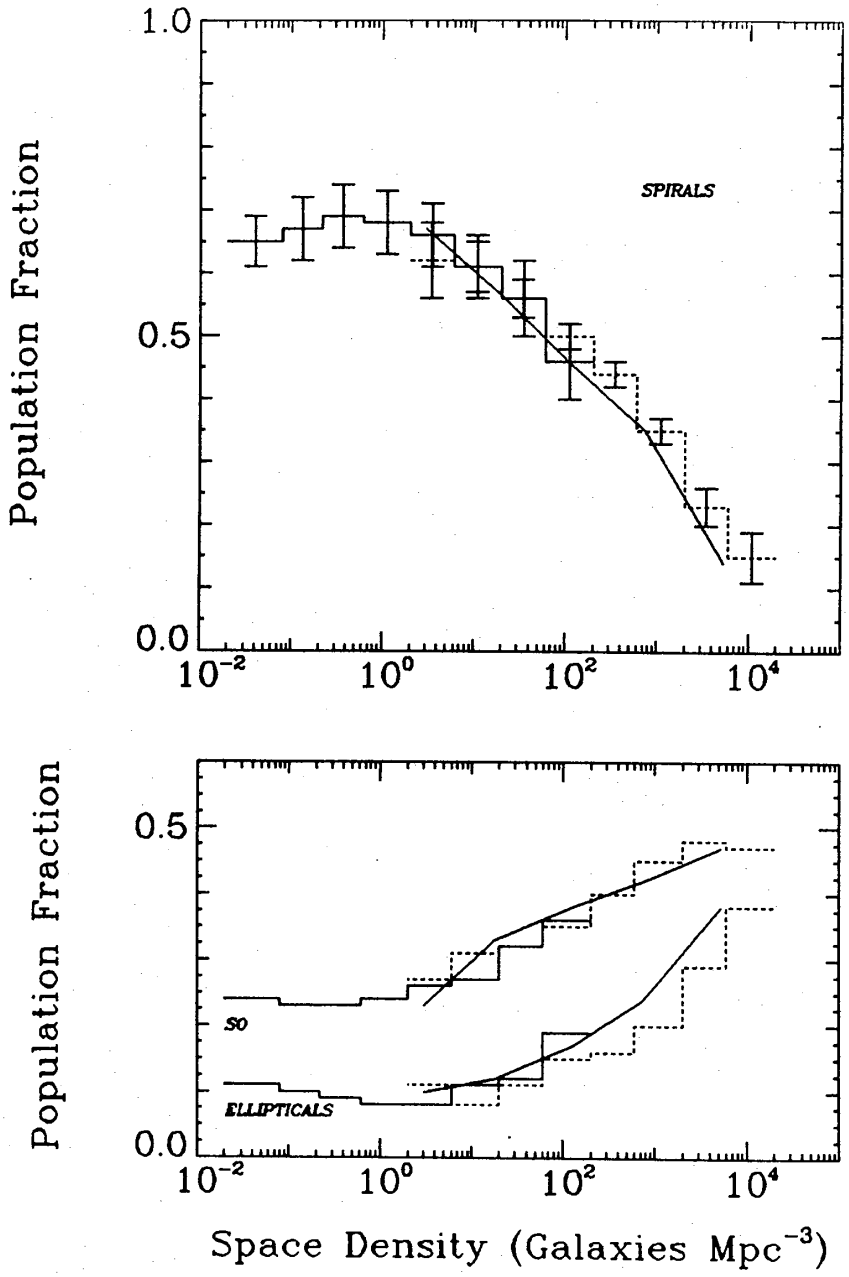

FIG. 1.—Population fraction as a function of space density for the CfA sample. The group contribution to the morphology-density relation is indicated by the solid histograms; the cluster contribution, by the dashed histograms. Dressler's morphology-density relation is indicated by the solid curves which are color corrected and shifted to correspond to $H_0 = 100$ km s^{-1} Mpc^{-1}.

Galaxy Spectral Energy Distributions

[Coleman, Wu, & Weedman 1980, *Ap.J. Supp,* **43,** 393]
[Fukugita, Shimasaku, & Ichikawa 1995, *Pub. A.S.P.,* **107,** 945]
[Kinney *et al.* 1996, *Ap.J.,* **467,** 38]
[Schmitt *et al.* 1997, *A.J.,* **114,** 592]

Galaxies of different types have different Spectral Energy Distributions, or SEDs. Consequently, the appearance of a galaxy can change with redshift. Its apparent luminosity will also vary, due to the fact that you are observing a different part of the its spectrum. This is called the K-correction. Note that K-corrections would occur even if a galaxy has a flat SED, since at higher redshift, one observes a smaller wavelength range (by a factor of $1+z$) through a finite bandpass filter.

The official definition of a K-correction is

$$K = 2.5\log(1+z) - 2.5\log\frac{\int_0^\infty I(\frac{\lambda}{1+z})S(\lambda)d\lambda}{\int_0^\infty I(\lambda)S(\lambda)d\lambda} \qquad (5.07)$$

where I is the flux from the object, and S is the throughput of the filter used for the observation. Note that there are two terms in the correction. The first occurs because a finite bandpass filter captures a smaller wavelength range of a galaxy; the second is a function of the galaxy's spectral energy distribution. Some authors are sloppy about including both terms, so watch out!

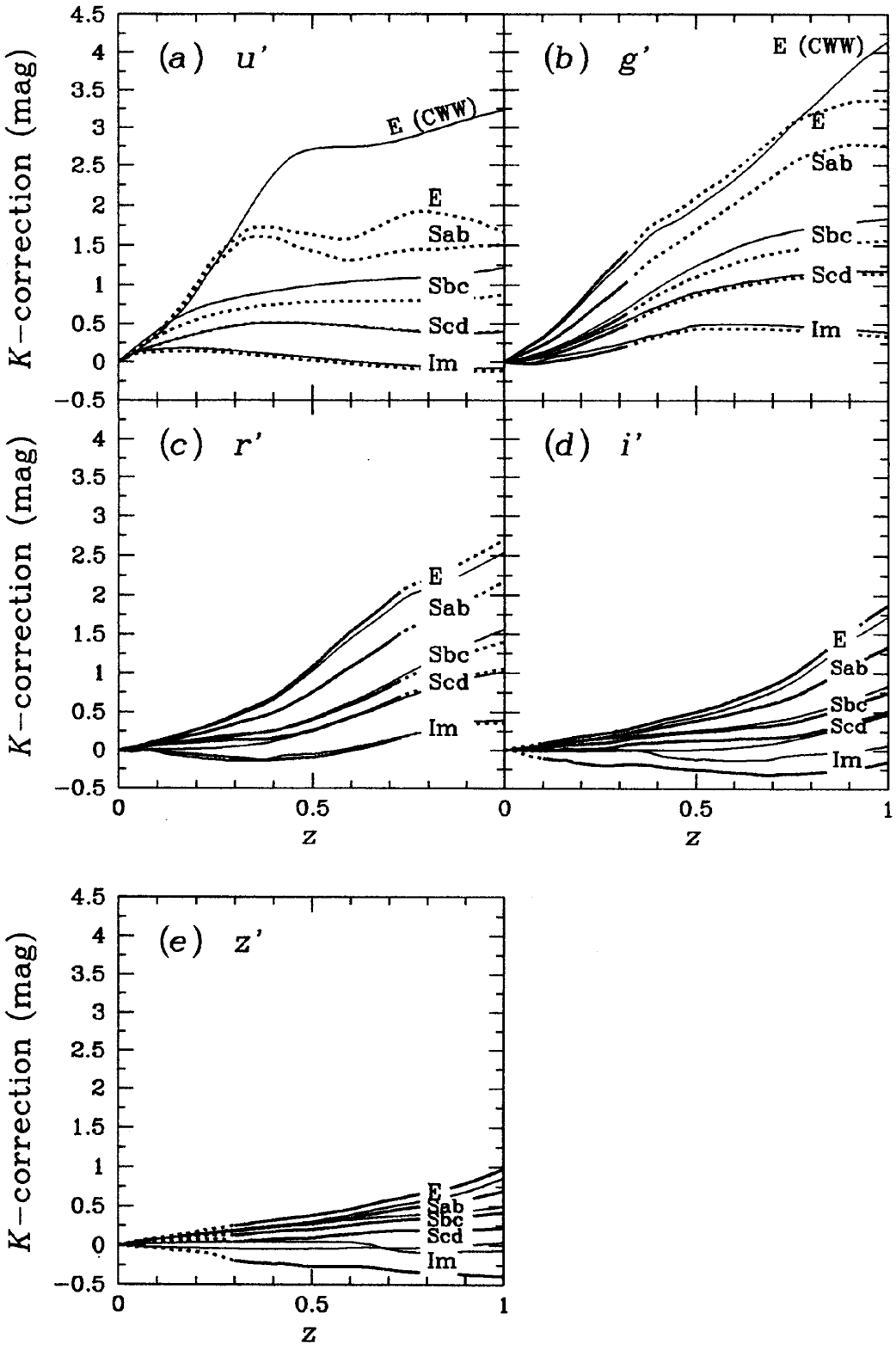

FIG. 20—*K* corrections for the SDSS photometric system. The meaning of curves is the same as that in Fig. 10.

Galaxy Clusters

[Abell 1958, *Ap.J. Supp.*, **3,** 211]
[Abell, Corwin, & Olowin 1989, *Ap.J. Supp.*, **70,** 1]
[Bahcall 1980, *Ap.J. (Letters)*, **238,** L117]
[Bautz & Morgan 1970, *Ap.J. (Letters)*, **162,** L149]
[Rood & Sastry 1971, *Pub. A.S.P.*, **83,** 313]

Most of the galaxies in the universe are not in clusters. Nevertheless, since these systems are the largest relaxed structures in the universe, their dynamical and evolutionary state can give us a handle on the condition of the universe as a whole. However, before we start going into the details of their structure, we should look at some galaxy cluster classification schemes.

For the very richest clusters, there is the system that George Abell devised. In the mid 1950s, as the original Palomar Schmidt Sky Survey was being completed, Abell eyeballed the plates, and identified the richest clusters in the sky. He then located the third brightest galaxy in the cluster, estimated its magnitude (m_3), estimated the brightness of a galaxy 2 magnitudes fainter than the third brightest galaxy ($m_3 + 2$), and, after estimating and subtracting off a background galaxy density, counted the number of galaxies with magnitudes between m_3 and $m_3 + 2$. The Abell Richness Class was then determined by the number of galaxies in this range.

Richness	# of Galaxies	Richness	# of Galaxies
0	30 - 49	3	130 - 199
1	50 - 79	4	200 - 299
2	80 - 129	5	> 300

In addition to assigning each cluster a Richness Class, Abell also assigned each a Distance Class (from 1 to 7). This was based on the assumption that the 10th brightest galaxy of each cluster is more-or-less a standard candle.

Because Abell noted down and published every cluster he spotted (before actually counting galaxies), his identifications are incomplete at the less-rich end. Therefore, only Abell Clusters with $R \geq 1$ and $|b^{II}| > 30^{\circ}$ are members of the "complete sample".

Note: the original Abell Clusters were defined only for that part of the sky accessible to the Palomar 48-in Schmidt telescope. In the early 1980s, Abell extended his work to the southern hemisphere via plates taken with the newly commissioned UK Schmidt 40-in telescope in Australia. (This photographic survey used finer emulsion than the original survey, but was otherwise identical.) Abell died before completing the catalog, but all 4073 clusters were eventually published in Abell, Corwin, & Olowin in 1989.

(By their very definition, Abell Clusters are the richest clusters in the universe. In 1980, Neta Bahcall wanted a way to describe poorer systems, so she just extended Abell's classification, so that $R = -1$ was equivalent to having between 20 and 29 galaxies between m_3 and $m_3 + 2$, $R = -2$ between 10 and 19 galaxies, and $R = -3$ for less than 10 galaxies.)

Complementing the Abell system is a morphological classification defined by **Bautz-Morgan** in 1970. This system describes how condensed a cluster is by the existence (or lack there-of) of a dominant (cD) galaxy. Clusters with a large, centrally located cD galaxy are classified as Bautz-Morgan I; clusters whose brightest galaxies are intermediate between a cD and a normal elliptical galaxy have the Roman numeral II, and clusters with no dominant galaxies are Bautz-Morgan type III systems.

Finally, there is the **Rood-Sastry** classification scheme, which seeks to organize the overall morphological properties of a cluster. These authors tried to use a tuning-fork diagram. At the base of the tuning fork are the regular, roughly spherical cD clusters. Binary clusters (type B) are next: these are similar to cD clusters, except that the cluster is dominated by two bright, central galaxies, rather than one. After type B, the tuning fork divides. On one side are the roughly spherical systems: C clusters, in which the bright galaxies are located near the cluster core, and I clusters, which are irregular in shape with no well defined center. On the other side of the tuning fork are L (linear) clusters, in which all the bright galaxies lie along a line, and F clusters, which appear as distinctly flattened systems.

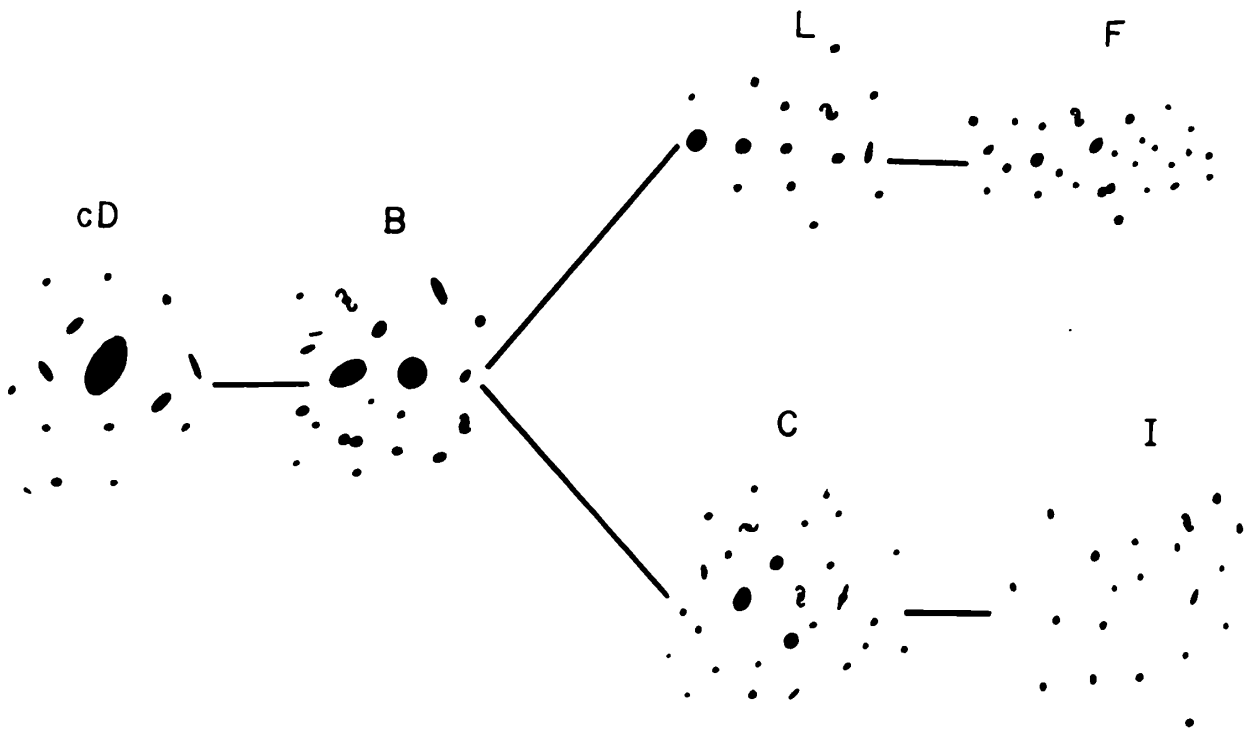

FIG. 1. — "Tuning fork" classification scheme for rich clusters of galaxies.

Part of what the cluster classification schemes are telling us is that not all clusters are alike, morphologically or dynamically. While some may be dynamically relaxed, others may just now be forming (and there are many cases where we believe two or more clusters are themselves beginning to merge). But sometimes it is difficult to tell the cases apart. In Virgo (which is equivalent to an Abell $R = 0$ cluster), the number counts and histogram of galaxy velocities both suggest that the cluster is virialized. However, when one looks at smaller velocity (or spatial) slices of the cluster, one see that the structure of Virgo is extremely complex and filled with substructure.